Anisotropic methanol transport in PMMA after mechanical deformation

Julie P. Harmon*, Sanboh Lee† and J. C. M. Li‡
Department of Mechanical Engineering, University of Rochester, Rochester, NY 14627, USA
(Received 8 September 1987; accepted 9 January 1988)

Transport of methanol in compressed PMMA (23–34% strain) was found to be anisotropic. It was faster by a factor of two to three in penetration velocity and by a factor of 10 in diffusivity in the direction of compression than in the perpendicular direction. However, the penetration velocity in the slow direction is still a factor of two to five larger than that of the undeformed PMMA (two at 40°C and five at 25°C). The two-dimensional mixed diffusion and case II transport problem was solved analytically so that the diffusivity and the penetration velocity could be obtained from experimental weight gain data. The penetration front was found to correspond approximately to a front of constant concentration of methanol. When methanol was mixed with glycerol to lower the methanol concentration (glycerol does not penetrate PMMA), the penetration velocity was smaller due to reduced swelling but the diffusivity was unchanged as expected.

(Keywords: PMMA; anisotropy; penetration velocity; diffusivity)

INTRODUCTION

Transport of small molecules in a polymer matrix is well known but not well understood. Both diffusion and swelling can take place. For very small molecules or very low solubility, swelling is not important and the diffusion is Fickian. For larger molecules or higher solubility, swelling can be so important that it controls the transport process. The penetrant front is sharp and moves with a constant velocity. It is known as the case II transport (case I being the Fickian diffusion). However, usually the process is neither case I nor case II.

Chau and Li[1] discovered that transport of methanol in PMMA shear bands is faster than that in the undeformed matrix. The transport process is Fickian in the shear bands and case II in the undeformed matrix. This observation prompted us to study the effect of mechanical deformation on penetrant transport[2,3]. Unlike the shear bands, the deformed PMMA shows a mixed behaviour, namely, a combination of case I and case II transport. A modified Kwei[4–8] equation was used to delineate the two processes. It was found that while at room temperature, the transport in the undeformed PMMA showed pure case II behaviour, it was mixed at higher temperatures (40–60°C). In all the cases, the deformed PMMA showed faster penetration and higher diffusivity than the undeformed at all the temperatures (35–60°C) studied.

During the course of these experiments, the transport along the direction of compression was found faster than that along a perpendicular direction. For thin slabs cut parallel to the compression axis, a sharp front swept across the face of the samples and extended much deeper than the sample thickness. On the other hand, for slabs cut perpendicular to the compression axis, a faint penetration front was observed on the face of the samples and disappeared early. This led us to believe that transport in deformed PMMA is anisotropic. Such behaviour and a two-dimensional transport model are reported in this paper.

MODEL FOR TWO-DIMENSIONAL TRANSPORT

Consider a parallelopiped sample of half-width a, half-thickness b and a long length dimension (*Figure 1*). When it is exposed in a penetrant environment such as liquid methanol, the penetrant enters in both width and thickness directions. The penetration in the length direction can be neglected so that the problem is essentially two-dimensional. The transport in each direction is assumed to obey the modified Kwei equation:

$$J_x = -D_1\frac{\partial C}{\partial x} - v_1(C - C_{0y}) \quad \text{for} \quad 0 \leqslant x \leqslant a \qquad (1)$$

$$J_y = -D_2\frac{\partial C}{\partial y} - v_2(C - C_{x0}) \quad \text{for} \quad 0 \leqslant y \leqslant b \qquad (2)$$

where C_{0y} is the concentration of penetrant at $(0,y)$ which varies with y but not x, C_{x0} is the concentration at $(x,0)$ which varies with x but not y, D_1 and D_2 are Fickian diffusivities and v_1 and v_2 are case II penetration front velocities for x and y directions, respectively. It is seen that equations (1) and (2) reduce to the simple two-dimensional diffusion if $v_1 = v_2 = 0$ and the simple two-dimensional case II transport if $D_1 = D_2 = 0$. They include all the various intermediate cases.

Equations (1) and (2) and the conservation of penetrant species require

$$\frac{\partial C}{\partial t} = D_1\frac{\partial^2 C}{\partial x^2} + D_2\frac{\partial^2 C}{\partial y^2} + v_1\frac{\partial C}{\partial x} + v_2\frac{\partial C}{\partial y} \qquad (3)$$

* Now at Kodak Research Labs, Rochester, NY 14650, USA
† Now at Department of Materials Science and Engineering, National Tsing Hua University, Hsinchu, Taiwan, ROC
‡ To whom correspondence should be addressed

0032-3861/88/071221-06$03.00

which can be solved using the following boundary conditions:

$$C = C_0 \text{ at } x = \pm a \text{ and any } y,t \tag{4}$$

$$C = C_0 \text{ at } y = \pm b \text{ and any } x,t \tag{5}$$

$$\frac{\partial C}{\partial x} = 0 \text{ at } x = 0 \text{ and any } y,t \tag{6}$$

$$\frac{\partial C}{\partial y} = 0 \text{ at } y = 0 \text{ and any } x,t \tag{7}$$

Initially the sample is free of penetrants. The concentration distribution at any time t is given by ($0 \leqslant x \leqslant a$, $0 \leqslant y \leqslant b$):

$$\frac{C}{C_0} = \sum_{n=1}^{\infty} \frac{p \sin(2\alpha_n a) \sin[\alpha_n(x-a)]}{S_1 + \cos^2(\alpha_n a)} \left[A_n + \sum_{m=1}^{\infty} \frac{v_2 S_2 \beta_m \sin[\beta_m(y-b)]}{\cos^2(\beta_m b)(S_2 + S_2^2 + \beta_m^2 b^2)} \frac{e^{-\gamma_{mn} t}}{\gamma_{mn}} \right]$$

$$+ \sum_{m=1}^{\infty} \frac{p \sin(2\beta_m b) \sin[\beta_m(y-b)]}{S_2 + \cos^2(\beta_m b)} \times \left[B_m + \sum_{n=1}^{\infty} \frac{v_1 S_1 \alpha_n \sin[\alpha_n(x-a)]}{\cos^2(\alpha_n a)(S_1 + S_1^2 + \alpha_n^2 a^2)} \frac{e^{-\gamma_{mn} t}}{\gamma_{mn}} \right] \tag{8}$$

where

$$p \equiv \exp\left[S_1\left(1 - \frac{x}{a}\right) + S_2\left(1 - \frac{y}{b}\right) \right] \tag{9}$$

$$S_1 \equiv v_1 a / 2D_1 \quad , \quad S_2 \equiv v_2 b / 2D_2 \tag{10}$$

$$\frac{2\alpha_n D_1}{v_1} = -\tan(\alpha_n a) \quad , \quad \frac{2\beta_m D_2}{v_2} = -\tan(\beta_m b) \tag{11}$$

$$\gamma_{mn} \equiv D_1 \alpha_n^2 + D_2 \beta_m^2 + \gamma \quad , \quad \gamma \equiv \frac{v_1^2}{4D_1} + \frac{v_2^2}{4D_2} \tag{12}$$

$$f_n^2 \equiv \frac{1}{D_2}(\gamma + D_1 \alpha_n^2) \tag{13}$$

$$g_m^2 \equiv \frac{1}{D_1}(\gamma + D_2 \beta_m^2) \tag{14}$$

$$A_n \equiv \frac{(f_n b)\cosh(f_n y) + S_2 \sinh(f_n y)}{(f_n b)\cosh(f_n b) + S_2 \sinh(f_n b)} \tag{15}$$

$$B_m \equiv \frac{(g_m a)\cosh(g_m x) + S_1 \sinh(g_m x)}{(g_m a)\cosh(g_m a) + S_1 \sinh(g_m a)} \tag{16}$$

The values of α_n, $n = 1,2\ldots$ and β_m, $m = 1,2,\ldots$ are positive roots for equation (11) and must be obtained numerically before substituting into equation (8).

Equation (8) can be integrated to obtain the total absorption at any time t

$$\frac{M}{M_\infty} = \sum_{n=1}^{\infty} \frac{\sin^2(2\alpha_n a)[1 - 2e^{S_1}\cos(\alpha_n a)]}{2S_1 b[S_2 + \cos^2(\alpha_n a)]} \left[C_n - \sum_{m=1}^{\infty} \frac{S_2 v_2 (\beta_m b)^2 [1 - 2e^{S_2}\cos(\beta_m b)]}{S_2(1+S_2) + (\beta_m b)^2} \frac{e^{-\gamma_{mn} t}}{\gamma_{mn}} \right]$$

$$+ \sum_{m=1}^{\infty} \frac{\sin^2(2\beta_m b)[1 - 2e^{S_1}\cos(\beta_m b)]}{2S_2 a[S_1 + \cos^2(\beta_m b)]} \left[D_m - \sum_{n=1}^{\infty} \frac{S_1 v_1 (\alpha_n a)^2 [1 - 2e^{S_1}\cos(\alpha_n a)]}{S_1(1+S_1) + (\alpha_n a)^2} \frac{e^{-\gamma_{mn} t}}{\gamma_{mn}} \right] \tag{17}$$

where

$$C_n \equiv b \frac{[(f_n b)^2 + S_2^2]\sinh(f_n b) + 2S_2(f_n b)[\cosh(f_n b) - e^{S_2}]}{(f_{1n} b)^2 [(f_n b)\cosh(f_n b) + S_2 \sinh(f_n b)]} \tag{18}$$

$$D_m \equiv a \frac{[(g_m a)^2 + S_1^2]\sinh(g_m a) + 2S_1(g_m a)[\cosh(g_m a) - e^{S_1}]}{(g_{2m} a)^2 [(g_m a)\cosh(g_m a) + S_1 \sinh(g_m a)]} \tag{19}$$

$$f_{1n}^2 \equiv \frac{1}{D_2}\left(\frac{v_1^2}{4D_1} + D_1 \alpha_n^2\right) \tag{20}$$

$$g_{2m}^2 \equiv \frac{1}{D_1}\left(\frac{v_2^2}{4D_2} + D_2 \beta_m^2\right) \tag{21}$$

The total amount of penetrant M_∞ at saturation is $4abC_0$ per unit length of sample.

EXPERIMENTAL

Materials and sample preparation

Crosslinked PMMA (Electroglas) contact lens buttons were obtained from Glasflex in Sterling, NJ. They were of standard size, 0.5 in. (12.7 mm) diameter and 0.187 in. (4.75 mm) thick. These buttons were stacked, fastened together with epoxy, mounted in a lathe and turned to a diameter of 5 mm. Discs (1.5 mm thick) were cut with a low-concentration diamond wafering blade. These discs were polished first on 400 and 600 grit carbimet paper (Buehler), and then annealed at 130°C for 12 h to relieve stresses. The annealed discs were compressed in an Instron to various loads between 20 kN and 60 kN at 0.001 mm s^{-1}. A control sample was left undeformed.

The deformed discs were mounted on chucks with epoxy and sliced either parallel or perpendicular to the compression direction. The control samples were also sliced in this manner. A Buehler isomet saw with a high-concentration diamond wafering blade was used to slice the samples. When the slices were perpendicular to the compression direction they were 0.4 mm thick and 5 mm in diameter. When they were parallel to the compression direction they were 0.4 mm thick, 1.0 mm wide and 5 mm long. Thickness measurements were made with a linear variable differential transformer (LVDT). Both thicknesses and widths were also measured by photomicroscopy.

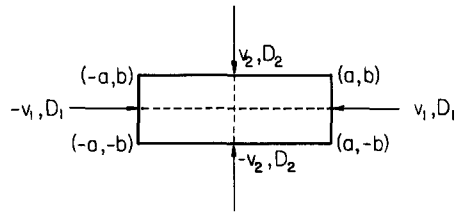

Figure 1 Schematic diagram for two-dimensional transport analysis. D_1, D_2 are diffusivities and v_1, v_2 are penetration velocities. All four are positive quantities

Temperature effects on two-dimensional transport

Slices cut either perpendicular or parallel to the compression axis were immersed in methanol at temperatures between 25°C and 40°C. Small holes were drilled near the ends of the slabs with a size 54 (0.055 in. or 1.4 mm) drill. Samples were suspended by copper wires and immersed in test tubes of methanol. Test tubes were placed in a Magni Whirl water bath accurate to ±0.2°C. After a specified period of immersion, samples were taken out of the methanol and weighed at intervals using the Perkin–Elmer AD-2Z autobalance. Some samples were observed at intervals in an Olympus microscope with transmitted light to reveal the penetration front. Photomicrographs were taken and the front measurements made from the negatives. A microscope grid with 0.01 mm spacings was used for magnification calibration.

Effect of compressive strain

The above procedure for weight gain measurements and penetration front observations was followed on samples subjected to different compressive strains. The temperature of the bath was 40°C for these experiments.

Effect of methanol concentration

Four specimen slices cut parallel to the compression direction were immersed in methanol–glycerine solutions made of 25, 50, 75 and 100% methanol by weight. USP glycerine was obtained from Purepac Pharmaceutical Company in Elizabeth, NJ. The bath temperature was 56°C. Gravimetric analysis was performed as described above.

DATA ANALYSIS

Penetration front measurement

Since the penetrant swells the polymer, the distance covered by the penetrant or moved by the penetration front was calculated from the unswollen dimensions of the sample as shown in *Figure 2*

$$d = a - x \tag{22}$$

where a is the unswollen sample half width. Both a and x were measured from the photomicrographs. The penetration distance in the thickness direction was calculated in the same way.

Two-dimensional analysis of sorption and penetration kinetics

Since transport was faster in the direction parallel to the deformation axis, slabs cut with the thickness direction parallel to this axis needed only one-dimensional analysis: v_1 and D_1 were then determined from equation (17) in reference 2 or equation (10) in reference 3 using the weight-gain data.

The two-dimensional equation (equation (17), was applied to the weight gain of slabs cut parallel to the deformation axis. The quantities v_1 and D_1, determined by one-dimensional analysis, were used so that D_2 and v_2 were then determined by curve fitting.

For case II sorption in undeformed and deformed samples (25°C), the sorption curve was calculated from the following equation:

$$\frac{M_t}{M_\infty} = \frac{ab - [(a - v_1 t)(b - v_2 t)]}{ab} \tag{23}$$

where M_t = weight gain at time t and M_∞ = equilibrium weight gain. For control samples, $v_1 = v_2$.

Two-dimensional concentration profiles were needed to determine the concentration at the penetration front visible in the microscope. Equation (8) was used with a constant value of $y/b = 0.005$ (0.005 was used instead of zero to facilitate computer calculations) and various values of x/a to calculate C/C_0. Plots of C/C_0 *versus* x/a were constructed for incremental times. This master plot allowed the determination of concentration at any distance and time.

RESULTS AND DISCUSSION

The effect of temperature on methanol sorption in two dimensions

The advancing penetration fronts in deformed and undeformed samples were sharp and clearly visible under the light microscope. The existence of sharp boundaries during case II transport is attributed to crazing[9,10] or a discontinuity in the diffusion coefficient[11]. Case II kinetics for undeformed sampls are summarized in *Table 1* and *Figures 3* and *4*. The temperature range is 25–40°C. At the higher temperatures, penetration velocities match the weight gain results. As the temperature is decreased, contributions from super-case II transport intervene. In addition, *Figure 4* shows penetration front measurements at 40°C for samples cut parallel and perpendicular to the

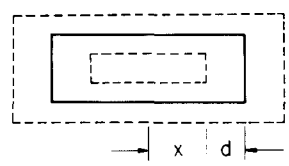

Figure 2 Schematic diagram showing the penetration front after swelling. The coordinates refer to the unswollen specimen

Table 1 Methanol absorption in undeformed PMMA slabs

Sample	T (°C)	v (from weight gain), 10^{-8} m s^{-1}	v (from penetration front), 10^{-8} m s^{-1}
N	25	0.13	0.2
L	30	0.28	0.4
J	35	0.65	0.6
H-1	40	1.03	1.2
H-2	40	–	1.2

Activation energy for case II transport = 25.3 kcal mol^{-1} = 106 kJ mol^{-1}

compression direction. The penetration curves are superimposable, demonstrating that the material is isotropic before deformation. The apparent activation energy for the case II process is 106 kJ mol^{-1} or 25.3 kcal mol^{-1}, which agrees with Windle's value of 25 kcal mol^{-1} for methanol transport in PMMA at lower temperatures[10].

For slabs cut with the thickness direction parallel (or the face perpendicular) to the compression axis, the weight gain data for sorption at different temperatures were fitted with the one-dimensional model as shown in *Figure 5*. For slabs cut with the thickness direction perpendicular (or the face parallel) to the deformation axis, the weight gain data were fitted with the two-dimensional model as shown in *Figure 6*. The penetration front travelling in the direction of compression extended well beyond the thickness dimension of the slab. *Table 2* lists the values of D_1, D_2 and v_1, v_2 from the fits. Transport is case II in both directions at 25°C.

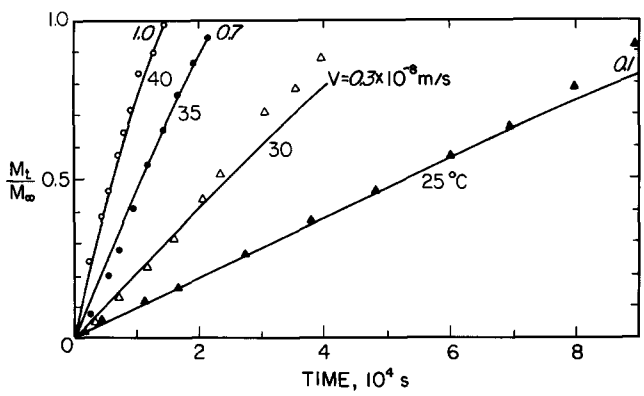

Figure 3 Methanol absorption in undeformed PMMA. Solid lines calculated from equation (23), the two-dimensional case II behaviour. Points are experimental

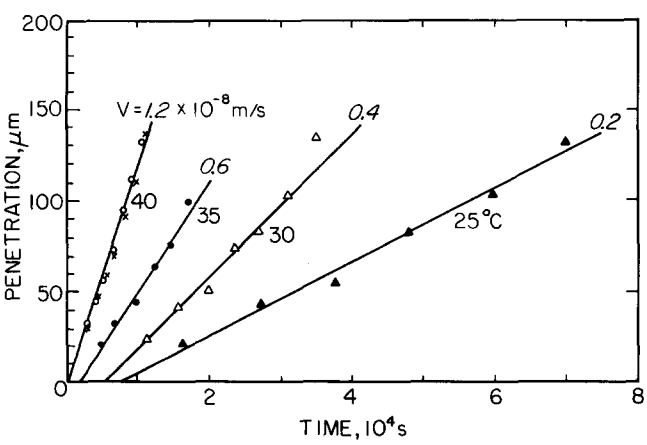

Figure 4 Methanol absorption in undeformed PMMA. Penetration front measurements at several temperatures

Penetration front measurements for slabs cut perpendicular to the compression axis showed that the concentration of methanol at the front was approximately constant as shown in *Figure 7*. Kwei *et al.*[6] observed penetration fronts during anomalous transport. A structural change must be responsible for the sharp front. When samples were removed before sorption equilibria had been reached, the sharp fronts remained in position long after desorption. A critical swelling stress may be needed for such structural change which is stable upon desorption but disappears upon further swelling.

The effect of plastic strain on methanol transport in two dimensions

Having determined that deformation induces anisotropic transport, the nature of this anisotropy was

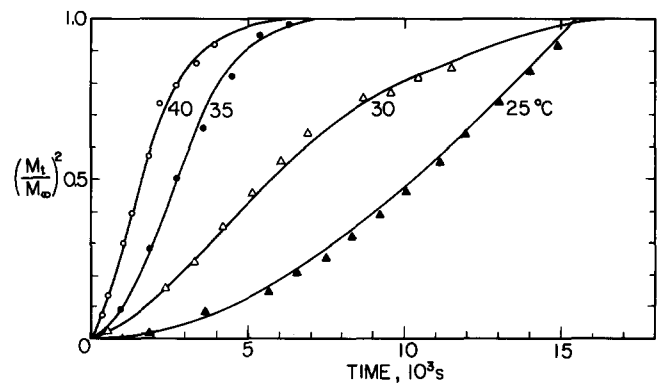

Figure 5 Methanol absorption in deformed PMMA slabs cut perpendicular to the compression direction. Solid curves calculated by fitting with a one-dimensional model except for the case of 25°C which was calculated from the one-dimensional case II behaviour. Points are expermental. D_1 and v_1 are listed in *Table 2*

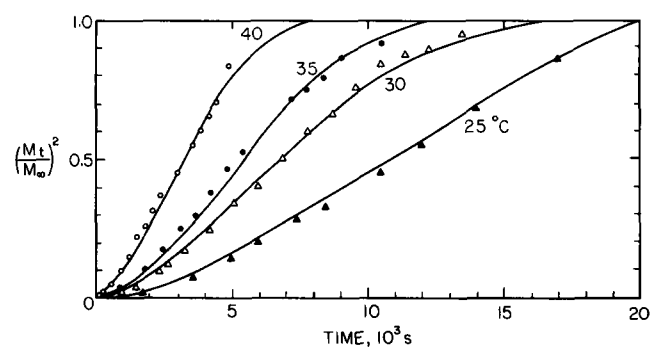

Figure 6 Methanol absorption in deformed PMMA slabs cut parallel to the compression direction. Solid curves calculated by fitting with the two-dimensional model (equation (17)), by knowing D_1 and v_1 from *Figure 5* and *Table 2*, except for the case of 25°C which was fitted with equation (23), the two-dimensional case II behaviour

Table 2 Methanol absorption in deformed PMMA slabs. The effect of temperature

Sample	T (°C)	v_1, 10^{-8} m s^{-1}	D_1, 10^{-12} m^2 s^{-1}	v^2, 10^{-8} m s^{-1}	D_2, 10^{-12} m^2 s^{-1}
M	25	1.6	–	0.7	–
K	30	2.2	1.0	1.2	0.1
I	35	5.5	1.0	1.2	0.1
A	40	7.0	3.0	2.5	0.2

investigated further by examining sorption and penetration in samples compressed to different strains. For crystalline polymers[12–15] a pronounced effect of per cent deformation or draw ratio on transport properties have been reported. Increases in transport kinetics during initial stages of drawing were attributed to rearrangements in the amorphous structure.

The present results, however, demonstrate that in the strain range of 23–34%, diffusion and relaxation both parallel and perpendicular to the compression axis are unaffected, as shown in *Table 3*. Case II transport was well defined at 0% strain where the sample was compressed to 20 kN but an anelastic strain remained after deformation. *Figure 8* shows that for this sample, sorption and penetration analysis defined a velocity of 2×10^{-8} m s^{-1} which is higher than that of the control, 1×10^{-8} m s^{-1}, at the same temperature. This reflects the fact that strain does not necessarily define the microstructural state. *Figure 9* shows that the penetration front corresponds to a constant concentration which depends on the compressive strain.

The effect of methanol concentration on sorption kinetics in deformed samples

To further investigate the nature of the front observed in deformed samples, the concentration of methanol was varied from 25 to 100% by weight as shown in *Figure 10*. At the higher concentrations, 100 and 75%, the diffusion coefficient remains unchanged, while swelling velocity decreases as methanol concentration decreases. The velocity is thus sensitive to the amount of swelling. When equilibrium solubilities decreased to 10% and lower, sorption tapered off after an initial rapid stage. These solubilities are near the levels observed at the fronts for 100% methanol.

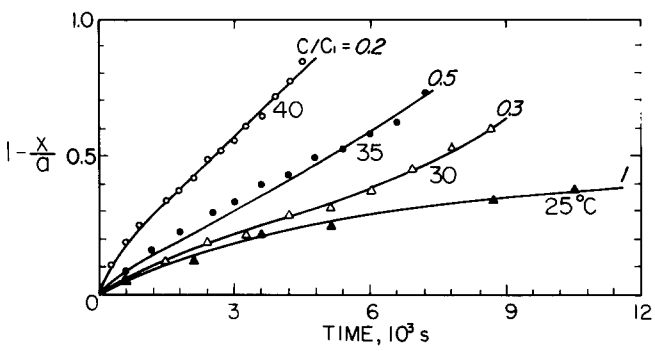

Figure 7 Methanol penetration in deformed PMMA slabs cut perpendicular to the compression axis. The penetration front movement was compared with the distance–time relation for a certain concentration

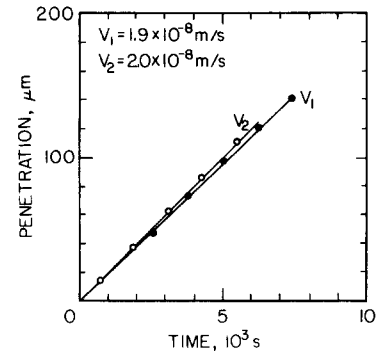

Figure 8 Methanol penetration in PMMA deformed without permanent strain. Transport was case II and isotropic but faster than the undeformed material

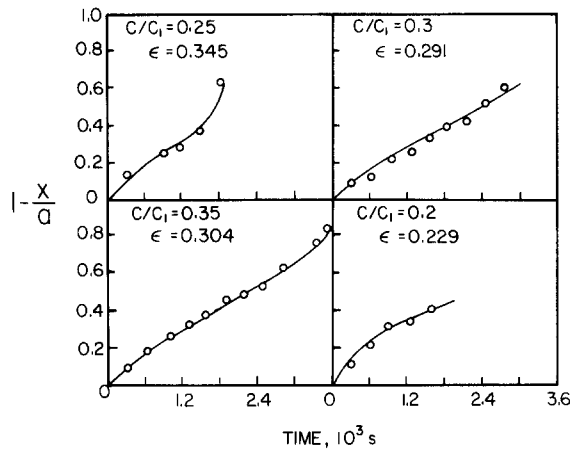

Figure 9 Methanol penetration in PMMA deformed to various plastic strains. Comparison of penetration front movement with distance–time relations for a constant concentration

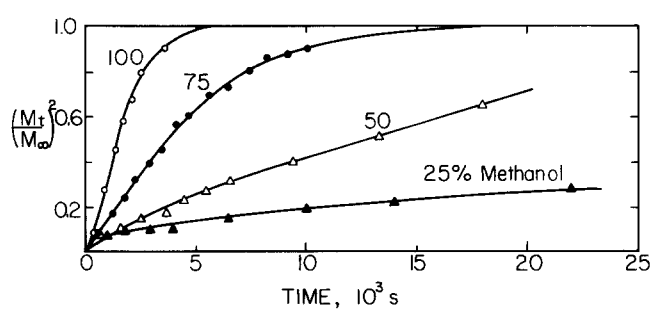

Figure 10 Effect of methanol concentration on the kinetics of methanol absorption in deformed PMMA slabs cut perpendicular to the direction of compression. See *Table 4*

Table 3 Diffusion and relaxation parallel and perpendicular to the compression axis

Sample	ε (%)	Load (kN)	D_1, 10^{-12} m^2 s^{-1}	v_1, 10^{-8} m s^{-1}	D_2, 10^{-12} m^2 s^{-1}	v_2, 10^{-8} m s^{-1}
A	38.4	60	3.0	7.0	0.2	3.3
B	34.5	50	3.0	7.0	0.2	3.6
C	30.4	45	3.0	7.0	0.2	2.5
D	29.1	40	3.5	7.0	0.2	3.5
E	22.9	35	3.0	7.0	1.0	6.0
F	5.4	25	–	–	–	–
G	0	20	–	1.9	–	2.0

v_1, D_1 ∥ to deformation axis; v_2, D_2 ⊥ to deformation axis

Table 4 Effect of methanol concentration on methanol absorption in defomred slabs (see *Figure 10*)

Methanol/Glycerol	Solubility (%)	$D, 10^{-12}\,m^2\,s^{-1}$	$v, 10^{-8}\,m\,s^{-1}$
100/0	22	3.8	7.5
75/25	15	3.8	2.0
50/50	10	–	–
25/75	4	–	–

CONCLUSIONS

For undeformed PMMA, methanol transport is isotropic and case II. The penetration velocity varies from $1.3 \times 10^{-9}\,m\,s^{-1}$ at 25°C to $1 \times 10^{-8}\,m\,s^{-1}$ at 40°C (pure case II) with an activation energy of $106\,kJ\,mol^{-1}$.

For deformed PMMA, methanol transport is anisotropic. The penetration velocity in the direction of compression varies from $1.6 \times 10^{-8}\,m\,s^{-1}$ at 25°C (pure case II) to $7 \times 10^{-8}\,m\,s^{-1}$ at 40°C, and that perpendicular to the direction of compression varies from $7 \times 10^{-9}\,m\,s^{-1}$ at 25°C (pure case II) to $2.5 \times 10^{-8}\,m\,s^{-1}$ at 40°C. The activation energy is about the same in the two directions, $70\,kJ\,mol^{-1}$, which is lower than that in the undeformed material. The diffusivity in the direction of compression varies from $10^{-12}\,m^2\,s^{-1}$ at 30°C to $3 \times 10^{-12}\,m^2\,s^{-1}$ at 40°C, and that perpendicular to the direction of compression varies from $10^{-13}\,m^2\,s^{-1}$ at 30°C to $2 \times 10^{-13}\,m^2\,s^{-1}$ at 40°C. The temperature range was not large enough to determine an activation energy. (The average is about $70\,kJ\,mol^{-1}$.)

The penetration front observable in the microscope seems to correspond to the location of constant concentration of the penetrant. However, since this concentration is not unique, the real reason for the sharp front must have a structural origin.

Methanol transport in PMMA deformed without a permanent strain is still isotropic and case II. However, the transport is faster than the undeformed material. After a critical compressive strain is imposed, sorption rates increase and then remain constant with further increase in strain.

Methanol diluted with glycerol causes less swelling of deformed PMMA. This effect reduces the penetration velocity but the diffusivity is not affected.

ACKNOWLEDGEMENTS

This work was supported partially by the ARO through grant number DAAG 29-80-0109 and partially by the DOE through grant number DE-FG02-85-ER45201. JPH acknowledges the receipt of an Allied Chemical Fellowship during the period 1978–80. Ms Jia Li checked some of the equations.

REFERENCES

1 Chau, C. C. and Li, J. C. M. *Philos. Mag.* 1981, **A44**, 493
2 Li, J. C. M. *Polym. Eng. Sci.* 1984, **24**, 750
3 Harmon, J. P., Lee, S. and Li, J. C. M. *J. Polym. Sci., (A) Polym. Chem. Ed.* 1987, **25**, 3215
4 Wang, T. T., Kwei, T. K. and Frisch, H. L. *J. Polym. Sci. A-2* 1969, **7**, 2019
5 Kwei, T. K., Wang, T. T. and Zupko, H. M. *Macromolecules* 1972, **5**(5), 645
6 Kwei, T. K. and Zupko, H. M. *J. Polym. Sci. A-2* 1969, **7**, 867
7 Wang, T. T. and Kwei, T. K. *Macromolecules* 1973, **6**, 919
8 Frisch, H. L., Wang, T. T. and Kwei, T. K. *J. Polym. Sci. A-2* 1969, **7**, 8
9 Hopfenberg, H. B. and Frisch, H. L. *J. Polym. Sci. B* 1969, 405
10 Thomas, N. L. and Windle, A. H. *Polymer* 1978, **19**, 256
11 Peterlin, A. *J. Res. Natl. Bur. Stand.* 1977, **81A** (2 & 3), 243
12 Peterlin, A. *J. Polym. Sci.* 1965, **69**, 61
13 Peterlin, A. *Polym. Eng. Sci.* 1977, **17**, 183
14 Peterlin, A. *J. Mater. Sci.* 1971, **6**, 490
15 Williams, J. W. and Peterlin, A. *J. Polym. Sci. A-2* 1971, **9**, 1483